Carbohydrate Polymers 111 (2014) 788–796

Contents lists available at ScienceDirect

Carbohydrate Polymers

journal homepage: www.elsevier.com/locate/carbpol

Removal of Cu(II) and Cr(VI) from wastewater by an amphoteric sorbent based on cellulose-rich biomass

Qian-Qian Zhong [b,*], Qin-Yan Yue [a,*], Qian Li [a,*], Bao-Yu Gao [a], Xing Xu [a]

[a] Shandong Key Laboratory of Water Pollution Control and Resource Reuse, School of Environmental Science and Engineering, Shandong University, Jinan 250100, PR China
[b] Tangshan College, Tangshan 063020, PR China

ARTICLE INFO

Article history:
Received 29 December 2013
Received in revised form 13 May 2014
Accepted 14 May 2014
Available online 27 May 2014

Keywords:
Biosorption
Cu(II)
Cr(VI)
Kinetics
Isotherms

ABSTRACT

A cellulose-rich biomass was modified as a new amphoteric sorbent to eliminate toxic Cu(II) and Cr(VI) from wastewater. The product (WSCA, which stands for modified wheat straw containing both cationic and anionic characters) presents high sorption capacities for the two ions which was evidenced by the comparison with unmodified wheat and other similar samples. Kinetic data and sorption equilibrium isotherms were conducted in batch process. The sorption kinetic analysis revealed that sorption of Cu(II) and Cr(VI) followed the pseudo second-order model well during the whole sorption process. The linear Langmuir isotherm model could perfectly describe the equilibrium data for Cu(II), while the sorption data of Cr(VI) were well fitted by the Freundlich. Results of the static test illustrated the complicated interactions between Cr(VI)/Cu(II) and WSCA including complexation and/or electrostatic attraction mechanisms.

1. Introduction

Water environment pollution has become a serious environmental problem worldwide, partly owing to the excessive emissions of heavy metal ion wastewater which have harmful effect on human physiology and other biological systems when they exceed the tolerance levels (El-Bayaa, Badawy, & AlKhalik, 2009). As a common heavy metal ion contaminant, copper(II) is widely used in many industries including metal cleaning and plating baths, paper board mills, wood pulp, paints and pigments, fertilizer industry and printed circuit board, etc. Accumulation of copper(II) in human body can cause liver and brain damage, stomach upset and ulcer, skin and heart diseases, and so on (Chen et al., 2010; Özer, Özer, & Özer, 2004; Zhu, Wang, & Chen, 2009).

Hexavalent chromium [Cr(VI)] is widely present in the effluents of electroplating, metal finishing, leather tanning and pigments industries (Liu, Zhang, Zhang, & Ren, 2012), which may pose a severe threat to public health because of their marked carcinogenic, teratogenic and mutagenic effects on human and other living organisms. Cr(VI) is primarily in the form of chromate (CrO_4^{2-}) and dichromate ($Cr_2O_7^{2-}$) ions and is known to be highly mobile, and much more toxic and hazardous than Cr(III). The maximum permissible level of Cr(VI) in potable water, inland surface water and industrial wastewater has been recommended by World Health Organization as 0.05, 0.1 and 0.25 mg L^{-1}, respectively (Chen et al., 2012).

Different treatment technologies have been developed for the purification of water/wastewater contaminated by heavy metals, including chemical precipitation, coagulation-flocculation, ion-exchange, membrane separation, reverse osmosis, solvent extraction, oxidation/reduction, electroflotation, etc. (Chen et al., 2010; Mohan & Singh, 2002). Amongst all the treatment processes mentioned, adsorption is a widely used and promising technique for sequestering toxic heavy metal ions from wastewater due to its high efficiency, flexibility in design, easy operation and avoidance of chemical sludge (Sud, Mahajan, & Kaur, 2008).

In recent years, numerous attempts have been made in finding inexpensive and effective adsorbents produced from agricultural and industrial solid waste. The advantage of using solid waste is that it reduces disposal costs while alleviating potential environmental problems (Zhu et al., 2009). Research on the agricultural waste materials—a kind of cellulose-rich biomass resources, modified by various methods for objective pollutants removal has generated much interest among researchers, environmental engineers and scientists. Low cost, wide availability, little content in non-fibrous materials, easy processing, and most importantly, many functional groups susceptible to chemical reactions contained. Due

* Corresponding authors. Tel.: +86 531 88365258; fax: +86 531 88365258.
E-mail addresses: zhqq.168@163.com (Q.-Q. Zhong), qyyue58@aliyun.com, qyyue58@yahoo.com.cn (Q.-Y. Yue), qianli@sdu.edu.cn (Q. Li).

http://dx.doi.org/10.1016/j.carbpol.2014.05.043
0144-8617/

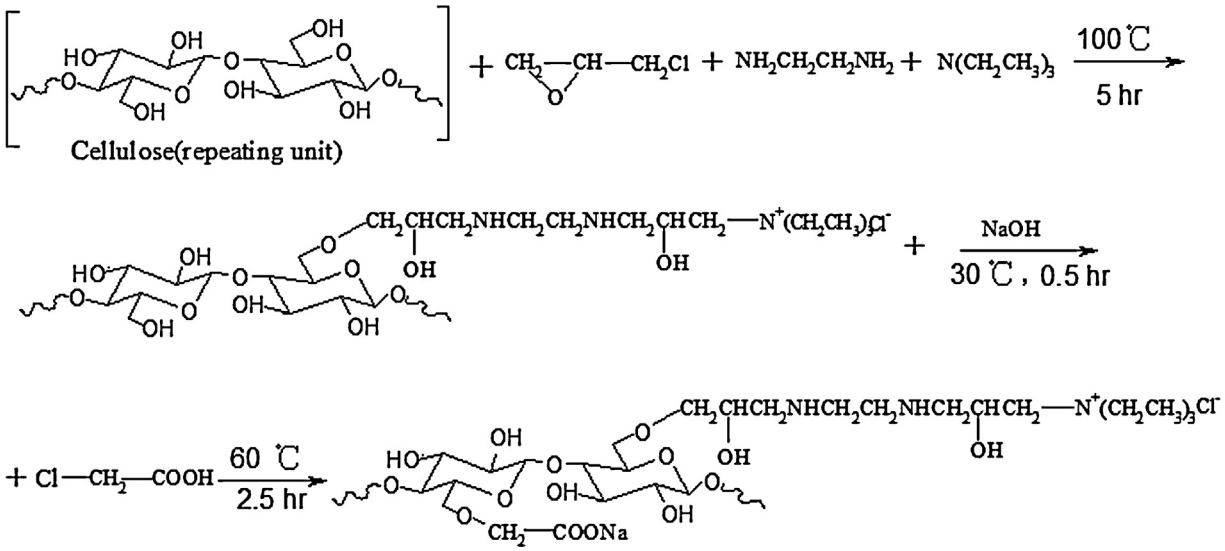

Fig. 1. Synthetic reactions for WSCA (cellulose as an example).

to all those advantages, cellulose based on biomass materials from renewable resource has attracted increasing attention. However, few studies were dedicated to the amphoteric biosorbents/resins, based on agricultural waste absorbent materials which can simultaneously eliminate anions and cations (Marshall & Wartelle, 2006; Zhu & Zhang, 2001). In addition, there has been no report on the sorption kinetics and isotherms studies for anions and cations onto the amphoteric biomass absorbents based on agriculture by-products.

In the present study, an amphoteric biosorbent (both amine and carboxyl contained) (WSCA) derived from wheat straw (WS) (a bio-based waste material) was used for the removal of Cu(II) and Cr(VI) from aqueous solutions. Physicochemical properties of WSCA were elucidated by SEM, XRD and IR analysis. The effect of pH, the isotherm and kinetic modeling in aqueous media were illustrated. Consequently, the objective of the work is as follows: (i) Providing theoretical ground for the research on application of other similar adsorption materials based on cellulose/lignin. (ii) Offering a probable explanation on adsorption mechanism.

2. Materials and methods

2.1. Preparation

The raw wheat straw was obtained from Jinan, China. It was washed with distilled water and dried at 105 °C for 24 h. Then the dried biomaterial was smashed and sieved to desired mesh size (380–500 μm) for use. The preparation of WSCA followed the procedures mentioned in our previous work (two separate two-step processes). Procedure 1: Two grams of wheat straw was reacted with epichlorohydrin (10 ml), ethylenediamide (4 ml), and triethylamine (10 ml) at 100 °C for 5 h (EET Method for short). Cellulose ether was formed after bridging and then quaternary amine groups were introduced onto the cellulose ether through cross-link. The intermediate product containing amine groups was synthesized.

Procedure 2: 6.69 g intermediate sample was reacted with NaOH (40%, w/w, 5 ml, 30 °C) and monochloroacetic acid (3.402 g, 60 °C) for 3 h. Carboxyl groups were transferred onto adjacent cellulose-repeating unit. The final product WSCA contained both amine groups and carboxyl groups was obtained (scheme was shown in Fig. 1) (Zhong, Yue, Gao, Li, & Xu, 2013).

2.2. Reagents

All the chemicals used in this study were of analytical grade (unless otherwise stated). Reagents for modification: epichlorohydrin, ethylenediamide and triethylamine. Chemicals for adsorption tests: Cu (spectrum pure grade), NaOH, HCl, HNO_3 (guaranteed reagent grade), $K_2Cr_2O_7$ (guaranteed reagent grade).

2.3. Physicochemical measurements

The physicochemical properties of WSCA were measured by SEM, XRD and IR. SEM micrographs of the virgin and modified samples were obtained by JEOL JSM-6480LV scanning electron microscope. The samples were coated with platinum before the SEM micrograph was obtained.

The functional groups present in raw wheat straw, WSCA, Cu(II)-adsorbed WSCA, Cr(VI)-adsorbed WSCA were investigated by the FT-IR analyzer (Thermo Nicolet Avatar 370, USA). Samples (5 mg) were encapsulated in 400 mg of spectroscopically pure KBr and the specimens were pressed into small translucent discs. IR spectra were obtained by averaging 60 scans from 4000 to 400 cm^{-1} region at 2 cm^{-1} resolution.

Crystallinities of WS and WSCA were determined by X-ray diffraction (XRD) using a diffractometer (X'TRA ARL) operated at 50 kV and 40 mA. The scanning scope and scanning speed was 5–55° and 5° min^{-1}, respectively, using CuKα radiation.

The pyrolysis behavior of WSCA was measured by thermogravimetric analysis (TGA) and differential scanning calorimetry (DSC) on a simultaneous thermal analyzer (SDT Q600). The sample weighed between 2 and 3 mg. The apparatus was continually flushed with dynamic nitrogen. The samples were heated at a rate of 10 °C min^{-1} from room temperature to 800 °C.

2.4. Adsorption tests

The pH effect experiments were performed at room temperature (20 °C) by adjusting the initial pH in the range of 2.0–6.0 for Cu(II) and 2.0–12.0 for Cr(VI) using 0.1 M HCl and NaOH. A dosage of 0.1 g WSCA was mixed with 50 ml of 50 mg L^{-1} Cu(II)/100 mg L^{-1} Cr(VI) solution in several 100 ml Erlenmeyer flasks. The suspensions were stirred for 120 min, filtrated by 0.45 μm of microfiltration membrane, and then equilibrium pH

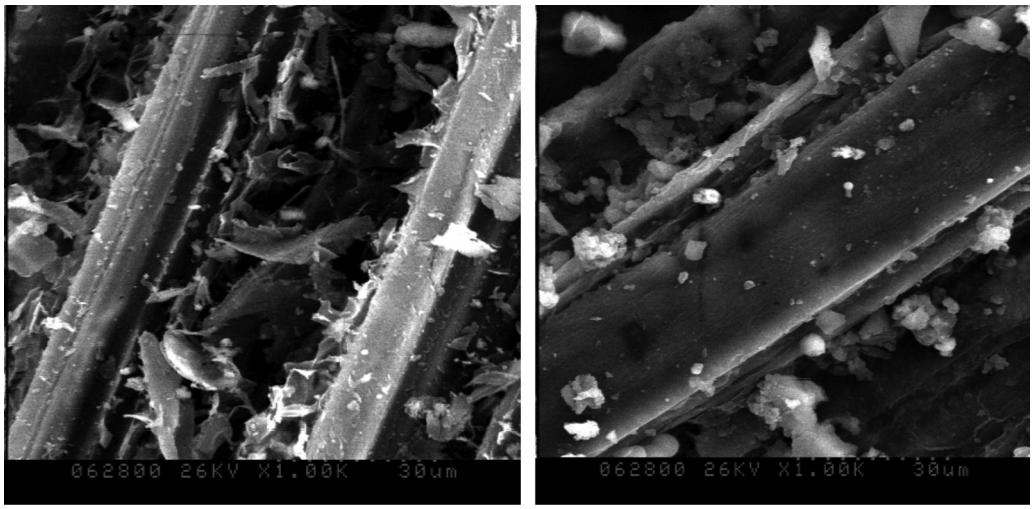

Fig. 2. SEM of (a) WS and (b) WSCA.

was determined. Samples were collected and filtered by 0.45 μm of microfiltration membrane. Cu(II) ions in the filtrate samples were detected at λ = 324.7 nm by atomic absorption spectrophotometer (TAS-990, Beijing Purkinje General Instrument Co. Ltd., China) with air-acetylene flame. The analyses of Cr(VI) in aqueous samples were conducted using a UV–visible spectrophotometer (model UV754GD, Shanghai) at λ = 540 nm after complexation with 1,5-diphenylcarbazide (Sun, Ma, Liu, Wang, & Gao, 2010).

Kinetic studies for Cu(II) were conducted using 0.1 g WSCA in 50 ml of the adsorbate solution [10, 25, 40, 50 mg L^{-1} for Cu(II) and 50, 80, 100, 150 mg L^{-1} for Cr(VI)] in 100 ml Erlenmeyer flasks. The suspensions were stirred at regular intervals [1, 5, 10, 20, 30, 45, 60, 90, 120, 150, 180, 240, 300, 360 and 420 min for Cu(II); 1, 5, 10, 20, 30, 45, 60, 90, 120, 150, 180 and 240 min for Cr(VI)]. The solution was filtered and then analyzed quantitatively, respectively.

Isotherm tests were performed to determine the maximum adsorption capacity (Q_{max}) for Cu(II)/Cr(VI) at different temperatures. WSCA (0.1 g) was mixed with 50 ml solutions in 100 ml Erlenmeyer flasks containing adsorbates with different initial concentrations [25, 50, 75, 100, 150, 200, 250, 300 mg L^{-1} for Cu(II) and 50, 100, 150, 200, 250, 300, 350, 400, 500, 600 mg L^{-1} for Cr(VI)]. The suspensions were stirred for 6 h and the temperature was monitored at 20, 30 and 40 °C.

3. Results and discussion

3.1. Physicochemical analysis

3.1.1. SEM surface morphology and XRD analysis

Fig. 2 shows the SEM of raw wheat straw and WS. It is obvious that the surface of WSCA was smoother than that of WS, which revealed that the order of cellulose was improved after removing the ash and extractives during the process of synthesis. As shown in Fig. 2(a), numbers of impurity particles were adhered to the surface of crude wheat straw, which was due to that there was a certain proportion of ash and extractives in addition to cellulose contained in original straw. The ash and extractives were multi-wrapped surface of the cellulose or lignin, while small amounts of which existed in non-crystalline region of the fiber. Therefore, the virgin straw surface was rough. In contrast, the amphoteric adsorbent had relatively smooth surface [as illustrated in Fig. 2(b)], which was due to the reaction of cellulose, hemi-cellulose, lignin during the process of synthesis, and most of the straw ash and extractives were removed, which made the order degree of fiber improve (Wang, Gao, Yue, & Yue, 2007; Xu, Gao, Yue, Zhong, & Zhan, 2010). In addition to this, no porous structure were observed on this surface. This structural feature of WSCA may be important because it illustrated the absence of porous adsorption in potential adsorption mechanism (Tan et al., 2012).

3.1.2. XRD analysis

The XRD diagrams of WS and WSCA are shown in Fig. 3. It is obvious that there are main and secondary peaks at 2θ of 22° and 16°, respectively, which is consistent with typical spectrum of cellulosic material. The main peak is taken as indicative of the presence of highly ordered crystalline cellulose, while the secondary peak stands for a less organized polysaccharide structure (Gong, Sun, Chen, Liu, & Yang, 2005). The heights of main peak and sub-peak both increase significantly in the diffraction curves of WSCA, indicating crystallinity of WSCA is actually increased compared with WS. Because a few impurities attached to the fibers have been removed during modification process and cause the improvement of the degree of crystallinity of WS, which is consistent with the research result of SEM. The increase in crystallinity

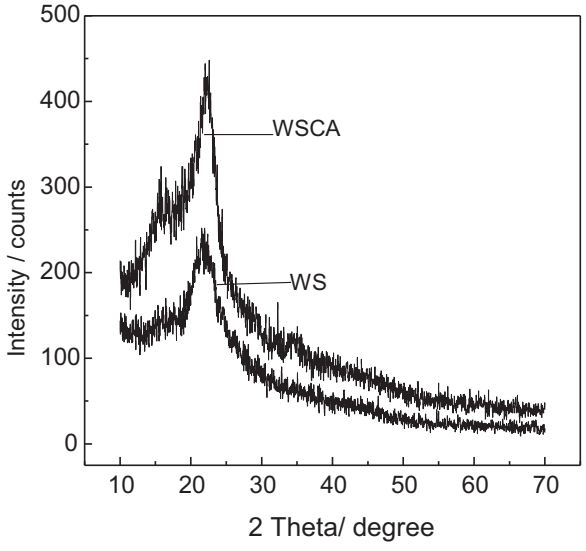

Fig. 3. XRD patterns of WS and WSCA.

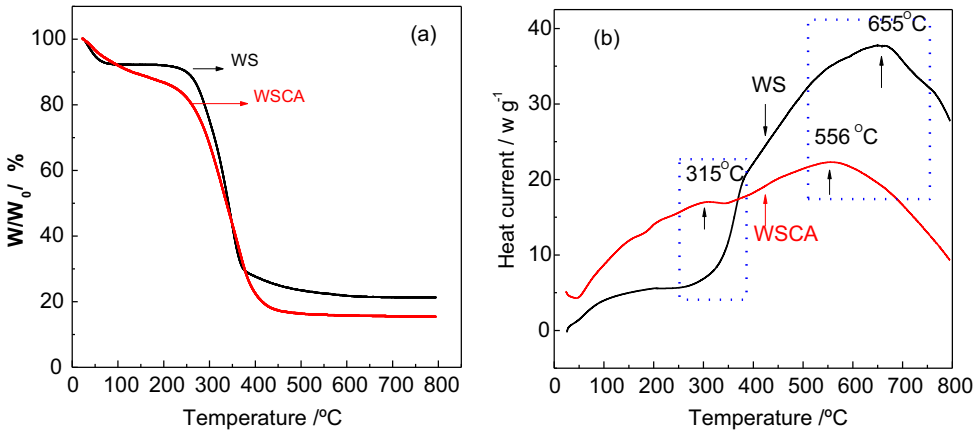

Fig. 4. TGA and DSC curves of WS and WSCA.

is associated with higher tensile strength of WSCA. Therefore the expected mechanical properties of the composite material could be improved by using WSCA.

3.1.3. Thermal stability

The thermal stability of WS and WSCA was determined by TGA and DSC. As shown in Fig. 4(a), the loss of weight during the TG analysis of WSCA and WS can be divided into three stages. The initial weight loss (~8% for WS and ~11% for WSCA) by heating the materials up to 150 °C has been due to the moisture elimination (Aravindhan, Rao, & Nair, 2009). The second stage of 150–400 °C corresponds to primary carbonization (Aravindhan et al., 2009; Yin et al., 2007), where there is a major weight loss (72.5% for WS and 77.4% for WSCA). The weight loss variation curve in this temperature range for WSCA shows a slight difference compared with WS, which suggests that the grafted chemicals have some effect on the pyrolysis behavior of WS to a certain extent. The third stage in 400–800 °C range indicates the decomposition of a structure with higher stability (Aravindhan et al., 2009).

For DSC curves, at around 655 °C and 556 °C exothermic peaks appeared for pristine straw and WSCA, respectively, which may contribute to the decomposition of cellulose and lignin in the materials (Sun, Xu, Sun, Xiao, & Sun, 2005); the main difference between the two curves in Fig. 4(b) was the exothermic peak at 315 °C for WSCA, compared with WS, which may be due to the decomposition of the grafted chemicals in WSCA.

3.1.4. FITR spectroscopy

Fourier transform infrared spectral analysis is important to identify some characteristic functional groups, which are responsible for sorption metal ions (Guo, Zhang, & Shan, 2008). Based on the attribution of peaks in the table, it can be known that WSCA contains a number of functional groups such as –OH, $–NH_2$, –COOH, etc.

As depicted in Fig. 5(a), (b) and Table 1, comparing WSCA with WS, the remarkable changes in corresponding peak wave number and shape, in the range 1367–1397 cm^{-1} and 1633–1651 cm^{-1} were assigned to the amine and carboxyl groups which appeared in the modified wheat, respectively (Guo et al., 2008; Gurgel, Melo, Lena, & Gil, 2009).

After Cu(II) sorption, significant changes have taken place for the characteristic peaks at 1051 cm^{-1} redshifted of 1043 cm^{-1}, which were corresponding to carboxyl after adsorption. The characteristic peaks at 1397 cm^{-1} redshifted of 1394 cm^{-1}, and the intensity of the peak dramatically changed to some extent corresponding to amino groups.

After Cr(VI) binding, the wavenumber of –OH group redshifted from 3445 cm^{-1} to 3422 cm^{-1}, indicating that complexation occurred considering the formation of surface complexes can affect the peak position of –OH (Chen et al., 2010). The characteristic peaks at 1397 cm^{-1} redshifted of 1386 cm^{-1}, corresponding to amino after adsorption. The peak at 1051 cm^{-1} blueshifted of 1055 cm^{-1}, and intensity of the peak dramatically weakened. This also verified the conclusion that carboxyl groups contributed to the sorption in a certain extent.

Overall, the carboxyl groups participated in sorption process for Cu(II), amino also contributed to the process to some extent. For Cr(VI), hydroxyl and amino contributed to the sorption process to a large extent, and carboxyl groups played a minor role. Based on the analysis, the mechanism of Cu(II) sorption onto WSCA was mainly due to the interaction between carboxyl groups and copper(II) ions; while for Cr(VI), hydroxyl and amino played a major role in the Cr(VI) binding as shown by the remarkable changes in corresponding peak wavenumber.

3.2. Adsorption tests

3.2.1. pH effect

pH is a deciding factor for any kind of metal sorption on sorbents in an aqueous solution (Hossain, Ngo, Guo, & Nguyen, 2012). The sorption of Cu(II) and Cr(VI) onto WSCA as a function of pH is shown in Fig. 6. Equilibrium pH values were also examined after the uptake of the two ions by WSCA at different initial pH.

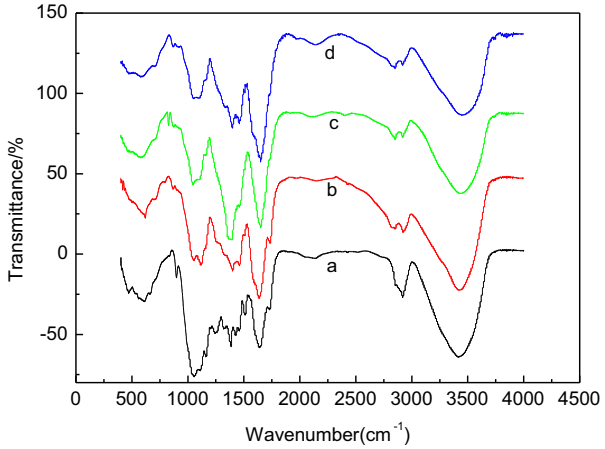

Fig. 5. FT-IR spectra of (a) WS, (b) WSCA, (c) WSCA-loaded Cu, and (d) WSCA-loaded Cr.

Table 1
Band position in the FT-IR spectra of WS, WSCA, WSCA-loaded Cu and WSCA-loaded Cr.

Frequency (cm^{-1})				Assignment	Reference
WS	WSCA	WSCA-loaded Cu	WSCA-loaded Cr		
3429.05	3444.49	3443.57	3421.76	–OH stretching	Huang et al. (2009)
2919.72	2915.01	2919.30	2928.43	C–H stretching	Guo et al. (2008)
2849.26	2849.57	2849.93	–	C–H stretching	Guo et al. (2008)
1632.75	1650.52	1651.03	1651.21	C=O stretching	Guo et al. (2008) and Gurgel et al. (2009)
1367.15	1397.15	1394.14	1386.53	N–H	
1050.66	1051.25	1043.30	1054.63	C=O stretching	Abdel-Nasser and El-Hendawy (2003) and Wang, Yang, et al. (2010)

For Cu(II) (Fig. 6(a)), it was observed that the variation tendency of the equilibrium pH is toward to the mid-range. When initial pH varied from 2 to 6, pH after adsorption was from 2.43 to 5.21.

Cu(II) removal increased with increasing solution initial pH. The hydrolysis products of copper as a function of pH are as follows: In the range pH 2–5, the dominant species of copper are Cu^{2+} and $CuOH^{+}$, above 6.3 the copper occurs as insoluble $Cu(OH)_2(s)$. At pH 6, there are three species: Cu^{2+} (in very small quantity), $CuOH^{+}$ and $Cu(OH)_2$ (in large quantity) (Benaïssa & Elouchdi, 2007).

The absence of sorption at low pH can be explained by the fact that at this acidic pH, the proton concentration is high and Cu(II) is present in solution as free cation (Cu^{2+} and $CuOH^{+}$), which can compete with protons for surface sites (Fiol et al., 2006). Whereas at higher pH fewer H^{+} ions compete with free cation, which suggests that heavy metal cations displace H^{+} from free hydroxyl of cellulose, hemicelluloses and lignin and –COOH groups introduced into the samples. Similar results were observed regarding the sorption of copper onto chemically modified aspen wood fibers (Huang, Ou, Boving, Tyson, & Xing, 2009).

For Cr(VI), a significant decrease in the equilibrium pH was observed compared with the initial pH values with range of 5.0–12.0. This could be attributed to the weakly acidic hydroxyl and carboxyl inherently in raw wheat and WSCA, which would decrease the solution pH in mild alkali conditions (Xu et al., 2011).

As depicted in Fig. 6(b), the uptake of Cr(VI) was almost constant at lower pH (2.0–3.0) and with pH increasing from 3.0 to 12.0, the sorption capacity of Cr(VI) decreased from 49.20 mg g^{-1} to 27.06 mg g^{-1}. The Cr(VI) in aqueous solution exists in various forms, such as $HCrO_4^{-}$, $Cr_2O_7^{2-}$, CrO_4^{2-}, etc. The yellow chromate anion, CrO_4^{2-} is predominant above pH 6.0, while $HCrO_4^{-}$ and $Cr_2O_7^{2-}$ are in equilibrium between pH 2.0 and 6.0 (Chen, Yue, Gao, Li, & Xu, 2011).

Sorption of Cr(VI) at lower pH suggested that the dominant species ($HCrO_4^{-}$) of Cr(VI) required one sorption site from the WSCA in order for the sorption to occur. In contrast, at high pH, the divalent forms of Cr(VI) species ($Cr_2O_7^{2-}$, CrO_4^{2-}) were mostly present and necessitated two sorption sites from WSCA for the sorption to occur (Yusof & Malek, 2009). This resulted in higher removal capacity of Cr(VI) species by WSCA at lower pH than at higher pH.

In addition, protonation and deprotonation of the amino groups grafted into WSCA may be contributed to the interaction mechanism. As illustrated by Eqs. (1) and (2), at lower pH, the protonation of sorbent surface was enhanced (Eq. (1)), and the positive charge on the surface of WSCA increased and thus attracted Cr(VI) with the negatively charged more strongly. At higher pH, OH^{-} ions may be adsorbed to the surface of the product, which contributed to the negatively charged surface sites of WSCA through hydrogen bonds (Eq. (2)). Then repulsion would exist between OH^{-} ions and Cr(VI), which decreased the sorption capacity of Cr(VI) (Sun et al., 2010; Zhong et al., 2013).

$$\text{Sur-NH}_2 + \text{H}^+ \rightleftarrows \text{Sur-NH}_3^+ \quad (1)$$

$$\text{Sur-NH}_2 + \text{OH}^- \rightleftarrows \text{Sur-NH}_2\cdots\text{OH}^- \quad (2)$$

where Sur denotes the surface of WSCA.

Besides, the binding of Cr(VI) ions with WSCA may be attributed to the partial conversion of Cr(VI) to the reduced form of Cr(III) on the surface of WSCA (Anandkumar & Mandal, 2009; Xu et al., 2011). There were three steps in the whole sorption process (Xu et al., 2011): (i) the binding of anionic ($HCrO_4^{-}$) Cr(VI) to the positively-charged groups (e.g. amine groups) present on the surface of WSCA (Eq. (3), (ii) the reduction of adsorbed Cr(VI) into Cr(III) by adjacent electron-donor (C=O, O–CH_3) groups (Eq. (4))

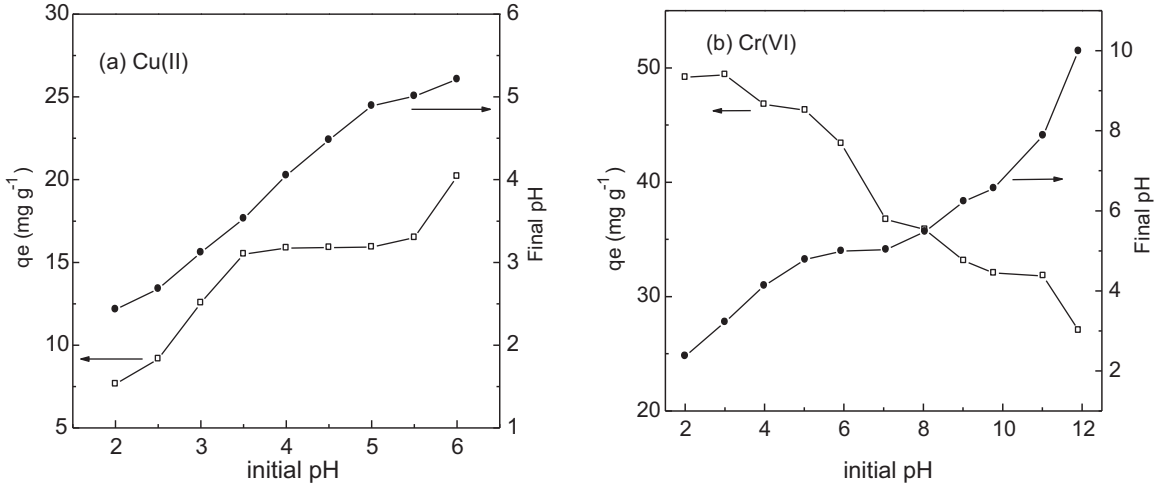

Fig. 6. Effect of initial solution pH on the sorption of Cu(II) and Cr(VI) onto WSCA and pH values before and after sorption [WSCA dosage: 2 g L^{-1}; T = 20 °C; shaking speed: 180 r min^{-1}; solution concentrations: 50 mg L^{-1} for Cu(II), 100 mg L^{-1} for Cr(VI); contacting time: 2 h].

and (iii) the complexation of the reduced-Cr(III) with adjacent groups, i.e. Cr-binding groups (Eq. (5)). Hydroxyl and carboxyl groups in biomaterials are suspected to bind anionic Cr(VI) ions with the aid of protons in aqueous phase:

$$\text{Sur-COOH} + \text{HCrO}_4^- + \text{H}^+ \rightarrow \text{Sur-COOH}_2^+\cdots\text{HCrO}_4^- \quad (3)$$

$$\text{Sur}^+\cdots\text{HCrO}_4^- + \text{H}^+ \rightarrow \text{Sur-oxidizedgroups} + \text{Cr}^{3+} + \text{H}_2\text{O} \quad (4)$$

$$\text{Sur–3(COOH)} + \text{Cr}^{3+} \rightarrow \text{Sur-3(COO}^-\text{)}\cdots\text{Cr}^{3+} + 3\text{H}^+ \quad (5)$$

Based on the above, it is suggested that the sorption mechanisms for Cr(VI) onto WSCA could be related to the complicated interactions including electrostatic attraction, complexation, ion exchange and so forth (Anandkumar & Mandal, 2009).

3.2.2. Kinetic studies

The adsorption capacities of WSCA for chromium (VI) and copper (II) versus the contact time are shown in Fig. 7. It can be observed that the sorption process was extremely rapid during the initial stage for all concentrations. This was attributed to the high concentration gradient in the beginning which exhibited a high driving force for the migration of chromium (VI) or copper (II) from solution to the surface of WSCA. Thereafter the rate of sorption was found to be slow and finally approached equilibrium. For 10 mg L^{-1} Cu(II), 4.7 mg Cu(II)/g WSCA was adsorbed after equilibrating for only 30 min. But for 25 mg L^{-1} Cu(II), 12.2 mg g^{-1} was adsorbed after 240 min and for 40 mg L^{-1} Cu(II), a maximum of 17.1 mg g^{-1} was adsorbed after equilibrating for 300 min. It is evident that an increase in the initial Cu(II) concentration led to a notable increase in the equilibrium time and sorption amount. Therefore, the sorption of Cu(II) by WSCA has a strong dependence on the initial concentration. Similar conclusions were drawn for the interaction between Cr(VI) and WSCA. Fig. 7(b) also illustrates a faster adsorption process and higher sorption capacity for chromium (VI) as compared to Cu(II). For 150 mg L^{-1} Cr(VI), 62.2 mg Cr(VI)/g WSCA was adsorbed after equilibrating for around 160 min.

Adsorption kinetics is proposed for the purpose of understanding the mechanism involved in the adsorption process. Numerous theoretical models provide an insight into the mechanism by which the adsorbate accumulates on the surface of the adsorbent (Gupta & Bhattacharyya, 2011). In order to appraise the adsorption kinetics of copper (II) and chromium (VI) onto WSCA, the experimental data were simulated by Lagergren pseudo-first order model (Eq. (6)), pseudo-second order model (Eq. (7)), Elovich equation (Eq. (8)) and intra-particle diffusion model (Eq. (9)) (Chen et al., 2011).

$$\ln(q_e - q_t) = \ln q_e - k_1 t \quad (6)$$

$$\frac{t}{q_t} = \frac{1}{k_2 q_e^2} + \frac{t}{q_e} \quad (7)$$

$$q_t = \frac{1}{\beta}\ln(\alpha\beta) + \frac{1}{\beta}\ln(t) \quad (8)$$

$$q_t = k_p t^{0.5} + C \quad (9)$$

where q_e and q_t (mg g^{-1}) are the amounts of the adsorbate sorbed per unit weight of sorbent at equilibrium and time t (min), respectively; k_1 (min^{-1}), k_2 (g (mg min)$^{-1}$), and k_p (g mg^{-1} $min^{-0.5}$) are the pseudo-first order rate constant, pseudo-second order equilibrium rate constant, and intra-particle diffusion rate constant, respectively; Elovich coefficients, α is the initial adsorption rate (mg (g min)$^{-1}$) and β is the de-sorption constant (g mg^{-1}) during any one experiment; C is the intercept, related to the thickness of the boundary layer.

The kinetic parameters under different conditions were summarized in Table 2. Pseudo-first order model showed correlation coefficients (R^2) of 0.9550–0.9785 for Cu(II) and 0.9005–0.9626 for Cr(VI); where as that of second-order kinetic model $R^2 > 0.995$ for Cu(II) and $R^2 > 0.999$ for Cr(VI) (figures are omitted). The insufficiency of the pseudo-first order model to fit the kinetics data could possibly be due to the limitations of boundary layer controlling the sorption process. Moreover, functional groups existing on the surface of WSCA such as hydroxyl, carboxyl and amine groups also all or partly contributed to the chemisorptions of Cu(II) and Cr(VI) onto WSCA in solutions, which was consistent with the conclusions in pH and IR analysis. The experimental data agree well with the pseudo-second order equation [correlation coefficient R^2 was observed to be close to 1 or equal to 1, which suggested that the process controlling the rate may be a chemical sorption involving valency forces through sharing or exchange of electrons between biosorbent and sorbate (Wang, Zhang, et al., 2010; Wang, Yang, et al., 2010; Zhu et al., 2009).

Diffusion from the solid–liquid interface to the interior of the solid particles plays a very important role in adsorption of metal ions. If the plots of q_t versus $t^{0.5}$ pass through the origin, the intra-particle diffusion will be the sole rate-limiting process. It is obvious that the plots did not have a zero intercept as proposed by Eq. (9) and Fig. 5(c) and (d). This indicates that although intra-particle diffusion is involved in the sorption process, it is not the only rate-limiting step, and boundary layer diffusion also controls the sorption to some degree; other kinetic processes are simultaneously occurring and contribute to the sorption mechanism (Zhu et al., 2009).

3.2.3. Adsorption isotherms

Temperature is an important parameter for the adsorption process. The sorption isotherms of Cu(II) and Cr(VI) onto WSCA are illustrated in Fig. 8. The batch experimental data were analyzed by Langmuir and Freundlich isotherm model equations and the models are represented mathematically as follows:

Langmuir equation:

$$\frac{1}{q_e} = \frac{1}{q_{\max}} + \left(\frac{1}{q_{maw} K_L}\right)\frac{1}{C_e} \quad (10)$$

Freundlich equation:

$$\ln\ q_e = \ln K_F + \frac{1}{n}\ln\ C_e \quad (11)$$

where q_e (mg g^{-1}) and C_e (mg L^{-1}) are the sorbate equilibrium concentrations in solid and the liquid phases; $q_{\max}$(mg g^{-1}), the monolayer capacity of the sorbent; K_L (L mg^{-1}) is a constant of the Langmuir isotherm. K_F (L g^{-1}) is Freundlich constant, and $1/n$ is the heterogeneity factor.

The theoretical parameters of isotherms along with regression coefficient are listed in Table 3. For Cu(II), the Langmuir model yields the better fit (R^2 = 0.9832–0.9843) compared to Freundlich equation, which shows the homogeneous nature of the sorbent by monolayer adsorption. Based on the Langmuir equation, the value of $q_{\max}$ increases with increasing temperature, and reaches 73.53 mg g^{-1} at 40 °C, which confirms that the sorption process for Cu(II) onto WSCA is an endothermic reaction. The n values of Freundlich model are in the range of 2–10, indicating a favorable sorption process, and similar results have been reported in the sorption of Cu(II) onto a new exchanger derived from tamarind fruit shell (Anirudhan & Radhakrishnan, 2008).

For Cr(VI), Freundlich isotherm gave a better description with higher R^2 value (>0.95), indicating that the applicability of a heterogeneous coverage of the Cr(VI) on the surface of adsorbent. Using Langmuir isotherm, the equilibrium data yielded the ultimate adsorption capacity value for WSCA, that is 227.3 mg g^{-1} at 40 °C.

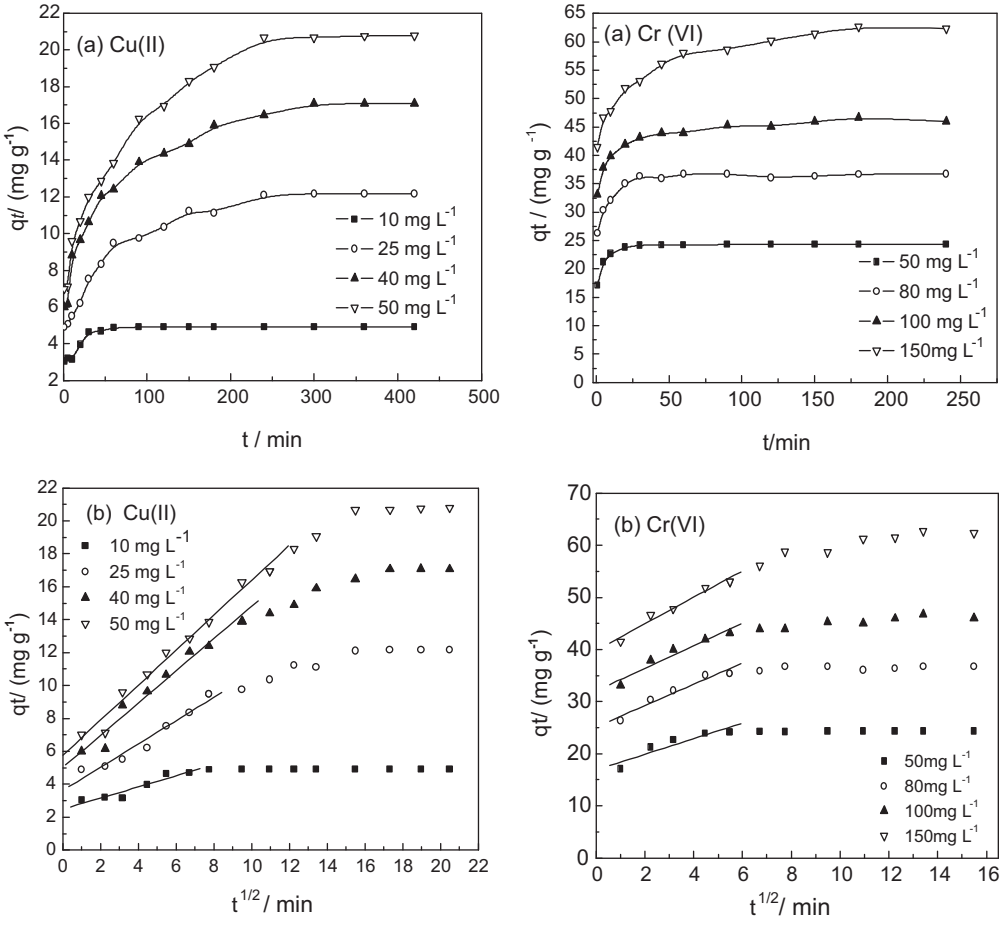

Fig. 7. (a) Effect of contact time on the uptake of Cu(II) and Cr(VI) by WSCA at different initial concentrations [WSCA dosage: 2 g L^{-1}; T = 20 °C; shaking speed: 180 r min^{-1}; pH: 4.0–4.5 for Cu(II), initial pH for Cr(VI)]; (b) intra-particle diffusion kinetics for sorption of Cu(II) and Cr(VI) onto WSCA at 20 °C.

Table 2
(a) Estimated kinetic model constants for Cu(II) adsorption. (b) Estimated kinetic model constants for Cr(VI) adsorption.

C_0 (mg L^{-1})	Pseudo-first order		Pseudo-second order		Elovich		Intra-particle diffusion	
	k_1 (min^{-1})	R^2	k_2 (g (mg min)$^{-1}$)	R^2	β (mg(g min)$^{-1}$)	R^2	k_p (mg (g min)$^{-1}$)	R^2
(a)								
10	0.05902	0.9593	0.08457	0.9999	2.616	0.8262	0.3387	0.8930
25	0.01388	0.9550	0.004587	0.9972	0.6576	0.9198	0.7076	0.9495
40	0.01378	0.9609	0.003247	0.9970	0.4603	0.9582	0.9792	0.9629
50	0.01197	0.9785	0.002128	0.9952	0.3584	0.9297	1.0632	0.9820
(b)								
50	0.0964	0.9525	0.08447	1	0.8536	0.7907	1.499	0.8540
80	0.0559	0.9213	0.02681	0.9999	0.5290	0.8908	2.044	0.9465
100	0.0226	0.9005	0.01103	0.9997	0.4140	0.9728	2.161	0.9375
150	0.0189	0.9626	0.004126	0.9994	0.2373	0.9759	2.543	0.9659

Table 3
Parameters obtained from Freundlich and Langmuir models.

Adsorbate	T (°C)	Langmuir				Freundlich		
		Q_{max} (mg g^{-1})	b (L mg^{-1})	R^2	R_L	K	n	R^2
Cu(II)	20	57.80	0.07665	0.9841	0.2069	13.83	3.697	0.9777
	30	69.93	0.1446	0.9843	0.1215	25.92	5.325	0.9485
	40	73.53	0.1609	0.9832	0.1106	29.04	5.663	0.9448
Cr(VI)	20	204.1	0.02469	0.9483	0.2883	28.92	3.127	0.9533
	30	222.2	0.03004	0.9181	0.2498	36.05	3.312	0.9541
	40	227.3	0.03813	0.9185	0.2078	38.70	3.237	0.9576

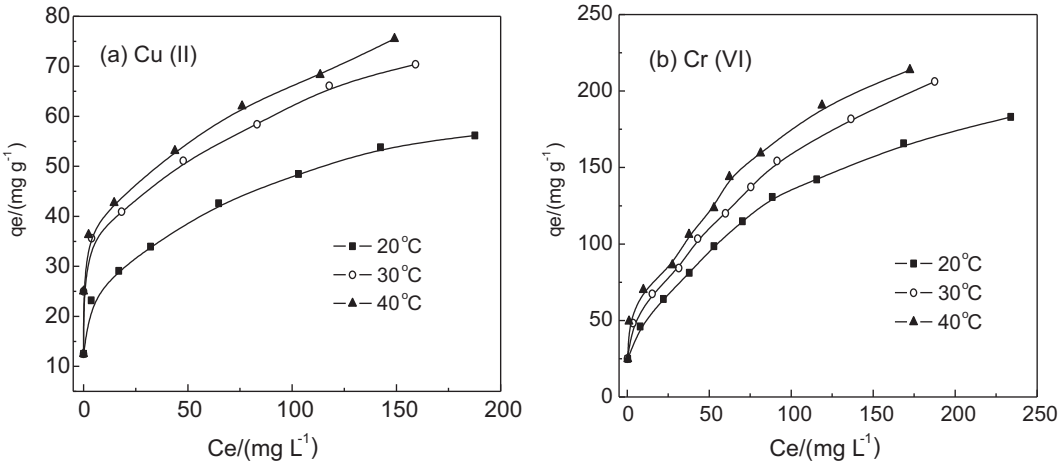

Fig. 8. Sorption isotherms of Cu(II) onto WSCA(WSCA dosage: 2 g L^{-1}; shaking speed: 180 r min^{-1}; pH: 4.0–4.5 for Cu(II), initial pH for Cr(VI).

3.3. Comparison for different modified products and discussions of research results

In this part, four modified products based on wheat by introducing cation and/or anionic groups with different orders were obtained. Produce yields and the amount of Cu(II) or Cr(VI) adsorbed by WSCA at a high loading of 80 mg L^{-1} of Cu(II)/200 mg L^{-1} of Cr(VI) are illustrated in Table 4. Product yields are above 100% for all samples, which is due to that the addition of reactants to the base material exceeds the loss of virgin material at the washing steps.

The sorption values for Cu(II) or Cr(VI) were recorded at a high loading of cation or anion, sufficient to saturate the binding sites for the sorbents (Table 4). However, these values represent an approximation of the adsorption capacity and true sorption capacities are obtained from sorption isotherms and the application of an appropriate mathematical model.

The product modified by chloroacetic acid (CA) had higher adsorption capacity for Cu(II) and slightly increased capacity for Cr(VI) compared with original straw, which is easily understood since exposure to chloroacetic acid imparts anionic character to the product. The increase in binding of Cu(II) cation may be due to the strong electrostatic interaction that occurred on the adsorbent surface.

The addition of amine groups to the CA-modified by-products further increased Cu(II) binding and the product had a much higher sorption capability for Cr(VI) over chloroacetic acid modification. This may be due to the strong electrostatic interaction between cationic groups (amine groups) and Cr(VI); while the increasing of adsorption capacity for Cu(II) was probably due to chelation between grafted amine groups and Cu(II).

When non-modified by-products are reacted with amine, there is a considerable increase in Cu(II) and Cr(VI) sorption. It results from the exposure to amine groups that imparts cationic character to the product, which causes electrostatic adsorption for Cr(VI) and chelation for Cu(II) to a large extent.

After the addition of chloroacetic acid (CA) to samples modified with amine, the products had lower adsorption capacity for Cr(VI) compared to samples modified with amine only, but resulted in a large increase in copper ion binding. Competition for the primary alcoholic hydroxyl (–OH) group on the C-6 carbon of glucose contained within the cellulose repeating units of the by-products contributed to the results. Due to reaction sites competition, carboxyl groups after being grafted had effect on amine groups previously grafted.

The order of by-product modification appears to influence ion binding in most cases. When CA is added first, Cr(VI) binding is higher than when CA is added last. When CA is added last, copper ion binding is higher than when CA is added first in most cases. Therefore, the modified group added last had greater advantage for the sorption efficiency of modified production. Similar results were observed for the research on dual-functional ion exchange resins prepared from by-products (Marshall & Wartelle, 2006).

The products discussed above were compared with a set of cellulose-based products which can both remove Cu(II) and Cr(VI) and commercial synthetic ion exchange resins for the adsorption of chromate ion or copper ion. Although these data were obtained under different experimental conditions, they will still be useful

Table 4
Adsorption of Cu(II) or Cr(VI) in aqueous solutions by various non-modified and modified products.

Sample	Product yield (%)	q_{max} (mg g^{-1})	
		Cr(VI)	Cu(II)
Raw wheat straw (WS)	NA	30.94	16.01
Anionc wheat straw (amine modified only)	545	257.35	72.85
Cationic wheat straw (CA-modified only)	108	32.24	33.35
Amphoteric wheat straw (CA-modified, then amine added)	461	270.13	65.12
Amphoteric wheat straw (amine modified, CA added)*	567	241.13	90.9
Dual-functional ion exchange resins (Marshall & Wartelle, 2006)	109–132	29.64–45.76	40.32–77.44
Amphoteric sugarcane bagasse cellulose (Zhu & Zhang, 2001)	NA	116.7	29.12
Amberlite IRC 748 (cation) (Lin & Juang, 2005)	NA	–	47.36–61.44
Amberlite IRA-400 (anion) (Marshall & Wartelle, 2006)	NA	111.3	–

Amphoteric wheat straw (amine modified, CA added) * was applied in our research.
NA: not applicable.

as a criterion for comparing the adsorption capacities. As can be seen from Table 4, WSCA demonstrated high sorption capacities for Cu(II) and Cr(VI) that surpassed commercially available cation/anion exchange resins and previously reported amphoteric cellulose-based products.

4. Conclusions

This work investigated the physicochemical characters of WSCA and its sorption behaviors for Cu(II) and Cr(VI). The pseudo second-order model described the kinetic data well, revealing that chemical sorption occurred. The equilibrium data can be well defined by Langmuir isotherm model for Cu(II) and Freundlich isotherm for Cr(VI), respectively. The order of product modification seemed to slightly favor the functionality that was added last. That is, if positive charge was added last, the products sequestered more Cr(VI) than a comparable sorption where the positive charge was added first and vice versa. Electrostatic attraction was the major removal mechanism for Cu(II), while electrostatic attraction and complexation (chelation to be exact) could both contribute to the sorption of Cr(VI) onto WSCA.

Acknowledgments

This work was supported by Natural Science Foundation of Shandong Province (ZR2010EQ031), Universities Innovation projects of Jinan City (201303080), National Natural Science Foundation of China (50878121, 21007034), the Key Projects in the National Science& Technology Pillar Program in the Eleventh Five-year Plan Period (No. 2006BAJ08B05), and the Science and Technology Development Key Program of Shandong Province, China (No. 2006GG2206007).

References

Abdel-Nasser, A., & El-Hendawy, A. A. (2003). Influence of HNO_3 oxidation on the structure and adsorptive properties of corncob-based activated carbon. *Carbon*, *41*, 713–722.

Anandkumar, J., & Mandal, B. (2009). Removal of Cr(VI) from aqueous solution using Bael fruit (Aegle marmelos correa) shell as an adsorbent. *Journal of Hazardous Materials*, *168*, 633–640.

Anirudhan, T. S., & Radhakrishnan, P. G. (2008). Thermodynamics and kinetics of adsorption of Cu(II) from aqueous solutions onto a new cation exchanger derived from tamarind fruit shell. *The Journal of Chemical Thermodynamics*, *40*, 702–709.

Aravindhan, R., Rao, J. R., & Nair, B. U. (2009). Preparation and characterization of activated carbon from marine macro-algal biomass. *Journal of Hazardous Materials*, *162*, 688–694.

Benaïssa, H., & Elouchdi, M. A. (2007). Removal of copper ions from aqueous solutions by dried sunflower leaves. *Chemical Engineering and Processing: Process Intensification*, *46*, 614–622.

Chen, H., Dai, G. L., Zhao, J., Zhong, A. G., Wu, J. Y., & Yan, H. (2010). Removal of copper(II) ions by a biosorbent—*Cinnamomum camphora* leaves powder. *Journal of Hazardous Materials*, *177*, 228–236.

Chen, S. H., Yue, Q. Y., Gao, B. Y., Li, Q., Xu, X., & Fu, K. F. (2012). Adsorption of hexavalent chromium from aqueous solution by modified corn stalk: a fixed-bed column study. *Bioresource Technology*, *113*, 114–120.

Chen, S. H., Yue, Q. Y., Gao, B. Y., Li, Q., & Xu, X. (2011). Removal of Cr(VI) from aqueous solution using modified corn stalks: characteristic, equilibrium, kinetic and thermodynamic study. *Chemical Engineering Journal*, *168*, 909–917.

El-Bayaa, A. A., Badawy, N. A., & AlKhalik, E. A. (2009). Effect of ionic strength on the adsorption of copper and chromium ions by vermiculite pure clay mineral. *Journal of Hazardous Materials*, *170*(2–3), 1204–1209.

Fiol, N., Villaescusa, I., Martínez, M., Miralles, N., Poch, J., & Serarols, J. (2006). Sorption of Pb(II), Ni(II), Cu(II) and Cd(II) from aqueous solution by olive stone waste. *Separation and Purification Technology*, *50*, 132–140.

Gong, R. M., Sun, Y. Z., Chen, J., Liu, H. J., & Yang, C. (2005). Effect of chemical modification on dye adsorption capacity of peanut hull. *Dyes Pigments*, *67*, 175–181.

Guo, X., Zhang, S., & Shan, X. (2008). Adsorption of metal ions on lignin. *Journal of Hazardous Materials*, *151*, 134–142.

Gupta, S. S., & Bhattacharyya, K. G. (2011). Kinetics of adsorption of metal ions on inorganic materials: A review. *Advances in Colloid and Interface Science*, *162*, 39–58.

Gurgel, L. V. A., Melo, J. C. P., Lena, J. C., & Gil, L. F. (2009). Adsorption of chromium (VI) ion from aqueous solution by succinylated mercerized cellulose functionalized with quaternary ammonium groups. *Bioresource Technology*, *100*, 3214–3220.

Hossain, M. A., Ngo, H. H., Guo, W. S., & Nguyen, T. V. (2012). Palm oil fruit shells as biosorbent for copper removal from water and wastewater: Experiments and sorption models. *Bioresource Technology*, *113*, 97–101.

Huang, L., Ou, Z., Boving, T. B., Tyson, J., & Xing, B. (2009). Sorption of copper by chemically modified aspen wood fibers. *Chemosphere*, *76*, 1056–1061.

Lin, L. C., & Juang, R. S. (2005). Ion-exchange equilibria of Cu(II) and Zn(II) from aqueous solutions with Chelex 100 and Amberlite IRC 748 resins. *Chemical Engineering Journal*, *112*, 211–218.

Liu, W. F., Zhang, J., Zhang, C. L., & Ren, L. (2012). Preparation and evaluation of activated carbon-based iron-containing adsorbents for enhanced Cr(VI) removal: Mechanism study. *Chemical Engineering Journal*, (189–190), 295–302.

Marshall, W. E., & Wartelle, L. H. (2006). Chromate (CrO_4^{2-}) and copper (Cu^{2+}) adsorption by dual-functional ion exchange resins made from agricultural by-products. *Water Research*, *40*(13), 2541–2548.

Mohan, D., & Singh, K. P. (2002). Single-and multi-component adsorption of cadmium and zinc using activated carbon derived from bagasse-an agricultural waste. *Water Research*, *36*, 2304–2318.

Özer, A., Özer, D., & Özer, A. (2004). The adsorption of copper(II) ions on to dehydrated wheat bran (DWB): Determination of the equilibrium and thermodynamic parameters. *Process Biochemistry*, *39*, 2183–2191.

Sud, D., Mahajan, G., & Kaur, M. P. (2008). Agricultural waste material as potential adsorbent for sequestering heavy metal ions from aqueous solutions—A review. *Bioresource Technology*, *99*, 6017–6027.

Sun, J. X., Xu, F., Sun, X. F., Xiao, B., & Sun, R. C. (2005). Physico-chemical and thermal characterization of cellulose from barley straw. *Polymer Degradation and stability*, *88*, 521–531.

Sun, X. F., Ma, Y., Liu, X. W., Wang, S. G., & Gao, B. Y. (2010). Sorption and detoxification of chromium(VI) by aerobic granules functionalized with polyethylenimine. *Water Research*, *44*(8), 2517–2524.

Tan, X., Gao, B. Y., Xu, X., Wang, Y., Ling, J. Y., Yue, Q. Y., et al. (2012). Perchlorate uptake by wheat straw based adsorbent from aqueous solution and its subsequent biological regeneration. *Chemical Engineering Journal*, (211–212), 37–45.

Wang, L., Zhang, J., Zhao, R., Li, Y., Li, C., & Zhang, C. (2010). Adsorption of Pb(II) on activated carbon prepared from *Polygonum orientale* Linn.: Kinetics, isotherms, pH, and ionic strength studies. *Bioresource Technology*, *101*, 5808–5814.

Wang, Y., Gao, B. Y., Yue, W. W., & Yue, Q. Y. (2007). Preparation and utilization of wheat straw anionic sorbent for the removal of nitrate from aqueous solution. *Journal of Environmental Sciences*, *19*, 1305–1310.

Wang, L. Y., Yang, L. Q., Li, Y. F., Zhang, Y., Ma, X. J., & Ye, Z. F. (2010). Study on adsorption mechanism of Pb(II) and Cu(II) in aqueous solution using PS-EDTA resin. *Chemical Engineering Journal*, *163*, 364–372.

Xu, X., Gao, B. Y., Yue, Q. Y., Zhong, Q. Q., & Zhan, X. (2010). Preparation, characterization of wheat residue based anion exchangers and its utilization for the phosphate removal from aqueous solution. *Carbohydrate Polymers*, *82*, 1212–1218.

Xu, X., Gao, B. Y., Tang, X., Yue, Q. Y., Zhong, Q. Q., & Li, Q. (2011). Characteristics of cellulosic amine-crosslinked copolymer and its sorption properties for Cr(VI) from aqueous solutions. *Journal of Hazardous Materials*, *189*, 420–426.

Yin, C. Y., Li, J. B., Xu, Q., Peng, Q., Liu, Y. B., & Shen, X. Y. (2007). Chemical modification of cotton cellulose in supercritical carbon dioxide: synthesis and characterization of cellulose carbamate. *Carbohydrate Polymers*, *67*, 147–154.

Yusof, A. M., & Malek, N. A. N. N. (2009). Removal of Cr(VI) and As(V) from aqueous solutions by HDTMA-modified zeolite Y. *Journal of Hazardous Materials*, *162*, 1019–1024.

Zhong, Q. Q., Yue, Q. Y., Gao, B. Y., Li, Q., & Xu, X. (2013). A novel amphoteric adsorbent derived from biomass materials: Synthesis and adsorption for Cu(II)/Cr(VI) in single and binary systems. *Chemical Engineering Journal*, *229*, 90–98.

Zhu, C. S., Wang, L. P., & Chen, W. B. (2009). Removal of Cu(II) from aqueous solution by agricultural by-product: Peanut hull. *Journal of Hazardous Materials*, *168*, 739–746.

Zhu, J. L., & Zhang, M. J. (2001). *Preparation of amphoteric sugarcane bagasse cellulose and study of its exchange adsorption properties*. Tianjin: Tianjin University.